Unusual July 10, 1996, rock fall at Happy Isles, Yosemite National Park, California

Gerald F. Wieczorek* *U.S. Geological Survey, M.S. 955, National Center, Reston, Virginia 20192*

James B. Snyder *National Park Service, P.O. Box 577, Yosemite National Park, California 95389*

Richard B. Waitt *Cascades Volcano Observatory, U.S. Geological Survey, Vancouver, Washington 98661*

Meghan M. Morrissey *Department of Geology and Geological Engineering, Colorado School of Mines, Golden, Colorado 80401*

Robert A. Uhrhammer *Berkeley Seismological Laboratory, University of California, Berkeley, California 94720*

Edwin L. Harp *U.S. Geological Survey, M.S. 966, Box 25046, Denver Federal Center, Denver, Colorado 80225*

Robert D. Norris *U.S. Geological Survey, Department of Geophysics, Box 351650, University of Washington, Seattle, Washington 98195*

Marcus I. Bursik
Lee G. Finewood } *Department of Geology, State University of New York, Buffalo, New York 14260*

ABSTRACT

Effects of the July 10, 1996, rock fall at Happy Isles in Yosemite National Park, California, were unusual compared to most rock falls. Two main rock masses fell about 14 s apart from a 665-m-high cliff southeast of Glacier Point onto a talus slope above Happy Isles in the eastern part of Yosemite Valley. The two impacts were recorded by seismographs as much as 200 km away. Although the impact area of the rock falls was not particularly large, the falls generated an airblast and an abrasive dense sandy cloud that devastated a larger area downslope of the impact sites toward the Happy Isles Nature Center. Immediately downslope of the impacts, the airblast had velocities exceeding 110 m/s and toppled or snapped about 1000 trees. Even at distances of 0.5 km from impact, wind velocities snapped or toppled large trees, causing one fatality and several serious injuries beyond the Happy Isles Nature Center. A dense sandy cloud trailed the airblast and abraded fallen trunks and trees left standing. The Happy Isles rock fall is one of the few known worldwide to have generated an airblast and abrasive dense sandy cloud. The relatively high velocity of the rock fall at impact, estimated to be 110–120 m/s, influenced the severity and areal extent of the airblast at Happy Isles. Specific geologic and topographic conditions, typical of steep glaciated valleys and mountainous terrain, contributed to the rock-fall release and determined its travel path, resulting in a high velocity at impact that generated the devastating airblast and sandy cloud. The unusual effects of this rock fall emphasize the importance of considering collateral geologic hazards, such as airblasts from rock falls, in hazard assessment and planning development of mountainous areas.

INTRODUCTION

At 6:52 p.m. July 10, 1996, two large rock falls with a combined volume of between 23 000 and 38 000 m^3 broke loose from cliffs about 1 km southeast of Glacier Point and fell just seconds apart to the floor of Yosemite Valley, near Happy Isles, Yosemite National Park, California (Fig. 1). The timing of the impacts of the rock falls was recorded by seismographic stations as much as 200 km away in central California and western Nevada. We estimated the volume of the rock fall from visual estimates of the dimensions of the rock-fall release area calibrated by Global Positioning Satellite readings made from a helicopter by National Park Service observers. The source of the rock fall was an arch of exfoliating rock about 150 m long, ranging from 10 to 40 m high, and estimated to be between 6 and 9 m thick, the majority of which detached in two large blocks. These two blocks slid down a steeply inclined ramp or shelf and then fell on a ballistic trajectory about 500 m (vertical) before hitting the northern part of a talus slope at the base of a cliff above the Nature Center at Happy Isles. The remaining southern parts of the arch, which fell later that night and next morning (Snyder, 1996) slid down a chute and landed on the southern part of the talus (Fig. 2).

The impacts of the blocks generated atmospheric pressure waves resulting in a wind (hereafter, airblast) comparable in velocity to that of a tornado or hurricane. The airblast uprooted and snapped about a thousand trees within an area of ~0.13 km^2 extending from the impacts on preexisting talus out to a bridge over the Merced River at Happy Isles 540 m away. Falling trees damaged the Happy Isles Nature Center, crushed a snack bar, destroyed a bridge, killed a hiker, and seriously injured several others. Just after the airblast a billowy dense sandy cloud of pulverized rock descended from the impact site toward the nature center, abrading trees and depositing gravelly coarse sand. Dust from the cloud rose rapidly into the air and plunged the area near Happy Isles into darkness for some minutes.

*E-mail: gwieczor@usgs.gov.

GSA Bulletin; January 2000; v. 112; no. 1; p.75–85; 11 figures; 2 tables.

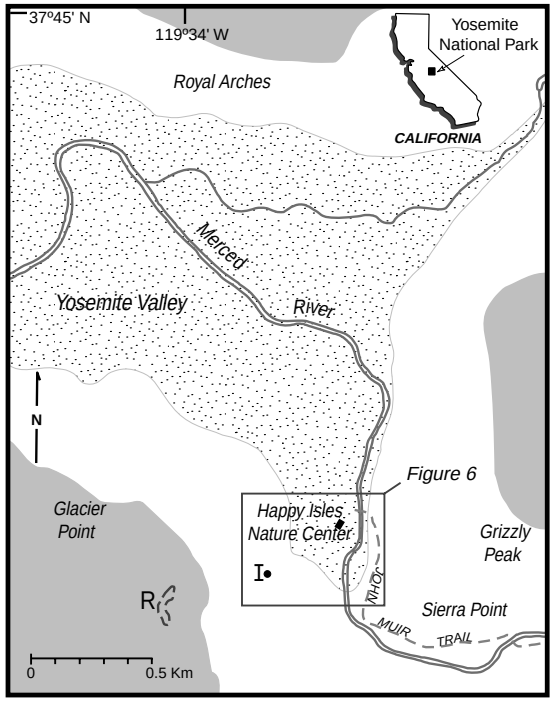

Figure 1. Location of Happy Isles rock fall in the east part of the Yosemite Valley, California. Rock-fall release (R) is shown by dashes and impact area (I) southeast of Glacier Point. Dark pattern indicates area that was above the most recent (Tioga) glaciation. Inset is map of California showing location of Yosemite National Park.

GEOLOGIC SETTING

Yosemite Valley is in the glaciated headward segment of the Merced River canyon in the central Sierra Nevada. Pleistocene glaciers deepened and broadened the valley. The source or release of the Happy Isles rock fall (1920–2000 m) was above the ~1767 m level of the ice at the maximum extent of the most recent (Tioga) major glaciation (Fig. 1; Matthes, 1930), ca. 20 ka (Alpha et al., 1987; Huber, 1987). Below this level of glaciation, the cliff is very steep and nearly devoid of vegetation. Above this level, the cliff is less steep and there is extensive root penetration into the jointed, weathered rock.

Extensive historic and prehistoric rock-fall deposits have accumulated at the base of the steep glaciated walls of the Yosemite Valley (Wieczorek et al., 1992). Earthquakes, rain storms, snowmelt, and freeze-thaw effects have historically caused rock falls in Yosemite, but more than half of the about 400 documented historical rock falls have occurred without a recognized or reported triggering event (Wieczorek and Jäger, 1996).

The Happy Isles rock fall occurred on a sunny day without an apparent triggering event such as an earthquake or storm. The preceding period had been relatively dry; only 16 mm of rain had fallen within the preceding 47 days. Heavy late melting winter snows supplied subsurface water draining toward the release well into the summer. A small amount of water continued to drain from joints in the release area during the day(s) following the rock fall. Even a small amount of water forming a column in a narrow crack or joint that does not freely drain can exert cleft pressure, reducing the stability of a rock mass. Black streaks of staining on the rock face indicate paths where water has historically seeped through the jointed rock mass. Seasonal discharge from a septic field upslope of the release possibly contributed to recharging ground water, but infiltration from rainfall and snowmelt creates natural seeps at many locations along the valley's cliffs. Seeps at the rock-fall release were draining at the end of the normally dry summer period in September 1998, even though the septic field had ceased operation by August 1997. Because the magnitude of pore-water pressures is difficult to assess at the release, the timing of the rock fall during a relatively dry period suggests that the role of pore-water pressure as a trigger of this rock fall is equivocal.

A combination of repeated cycles of freeze-thaw of water in joints, root penetration and wedging, or stress relief following deglaciation likely led to the gradual weakening and failure of the arch. The release of the arch probably initiated by sliding down the intersection of steeply inclined joints (Gilliam, 1998). A stand of pine and oak trees in earlier photos had grown along the joints defining the back of the arch; roots as thick as 20 cm had grown down into the joints. The roots may have wedged the arch apart as they penetrated deeper.

The arch-like rock mass involved in the Happy Isles rock fall event was composed of granodioritic and tonalitic rocks from a unit included in the Sentinel Granodiorite by Calkins (*in* Matthes, 1930), later mapped as the granodiorite of Glacier Point by D. L. Peck (1997, written commun.). Below the source area this granodiorite overlies the Half Dome Granodiorite along a sharp contact that dips steeply west.

Arches along the steep walls of Yosemite Valley develop as joint-bounded blocks break loose from beneath more massive, less jointed rock. Most arches collapse before becoming completely free standing. Collapse of developing arches on the valley walls produces large talus piles, as existed above Happy Isles before this rock-fall event. Historical photographs document several of the rock-fall events during the development of the arch above Happy Isles. The August 2, 1938, rock fall created much noise and dust and added considerably to the talus pile, yet caused no damage. A low ridge topped by large boulders near the Happy Isles Nature Center probably formed by a prehistoric rock fall (Fig. 2).

DYNAMICS OF ROCK FALL

Although the entire rock-fall event from release to impact was not observed, the process can be partially reconstructed from eyewitness accounts, seismographic recordings, field evidence, and calculations. The north wing of the arch collapsed first, breaking into two blocks (hereafter, blocks A and B) that slid about 235 m (slope distance) along a shelf before falling off the cliff (Fig. 3). Park Service interpreter Geoff Green saw two blocks falling within several seconds of each other from the rim southeast of Glacier Point. The mechanism of failure of the arch or the type(s) of movement the rock mass constituting the arch underwent as it collapsed before reaching the ramp are not known. Subsequent measurement of joint orientations in the release area combined with stereographic slope stability analyses indicate that toppling was not as likely to be the initial type of movement involved in collapse of the arch as sliding of blocks or wedges controlled by steeply dipping joint planes and/or joint intersections (Gilliam, 1998).

Rock falls have previously been recorded and recognized using seismic equipment (Norris, 1994); the impacts of blocks A and B at Happy Isles were recorded at 6:52 pm by seismographic stations as much as 200 km away. The second and larger impact had a local magnitude (M_L) of 2.15, determined from Wood-Anderson seismographs synthesized from recordings at the three closest broadband stations, which were within 80 km of Happy Isles (Uhrhammer, 1996). The prominent phases recorded on the record (Fig. 4) are consistent with two impacts 13.6 s apart, the amplitude of the second event about four times the amplitude of the first event.

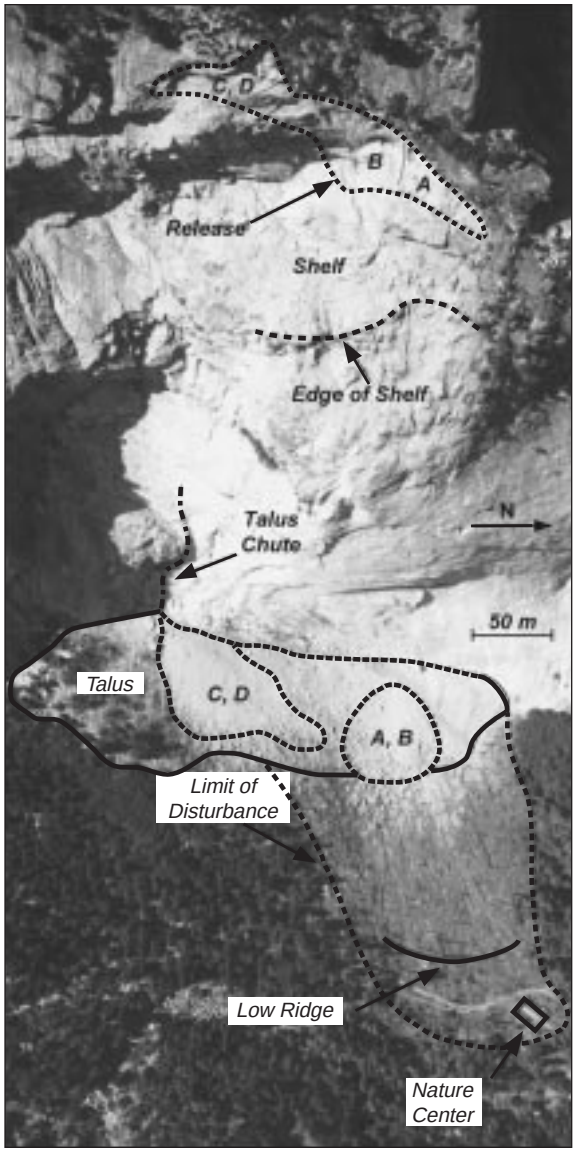

Figure 2. Rock-fall release (blocks A, B, C, and D), steeply inclined shelf, impact areas (A, B) (C, D) on talus, limit of disturbance by airblast and dense sandy cloud, low ridge of prehistoric rock fall, and nature center. Scale is approximate. Locations of release, impact area, and nature center shown in Figure 1. (Photograph by Pacific Aerial Surveys, September, 1996.)

During travel down the steep ramp, which averaged about 47º, the blocks gained sufficient horizontal velocity to clear the base of the steep cliff by 30–60 m (Fig. 5), which we measured by pacing in the field and locating on aerial photographs. The sequence and relative size of these two falling blocks was confirmed by inspection of the impact-area talus beyond the foot of the cliff. A low mound of freshly crushed and broken rock at the north edge of the talus indicates the impact of the first smaller block A. A larger disaggregated mass of rocks from the impact of the second, much larger, block B overlies the mound of rocky debris from block A to the southeast (Fig. 6A).

We calculated the velocity of the rock fall using the algorithm in the Appendix. The algorithm requires as input the cliff profile, the release elevation, the beginning of free fall elevation, and the valley floor elevation at impact. The algorithm numerically integrates the equations of motion in two dimensions (x, z) and it gives the position and related parameters of the center of mass every 10 ms. The release elevation of the approximate center of mass of block B (1940 m) was used in conjunction with a digitized profile along the path from release to impact taken from the contours of the 1:24,000-scale U.S. Geological Survey Half Dome topographic map. In order to simplify the algorithm, it is assumed that the block went ballistic at an elevation of about 1770 m, a break in slope corresponding to the former level of Tioga glaciation. From field and air photo observation, the center of impact B on the valley floor was about 480 m (±15 m) from the release, which corresponds to a position of x = 500 m (Fig. 5) because the profile begins 20 m west of the release. The impact occurred at an elevation of about 1275 m. If we assumed a frictionless surface for motion along the shelf with no air drag, the velocity at impact on the talus would be about 120 m/s with a total transit time (sliding and projectile) of about 12.4 s. An example of the output from the algorithm is given in Table A1.

The relatively high calculated velocity (70 m/s) of the block by the end of the ramp suggests that either the coefficient of friction must have been very low and/or that the block had an initial velocity. A short free fall of the collapsing arch onto the ramp might have imparted an initial velocity to the block before it commenced traveling down the steep ramp. The block could have moved down the ramp by sliding, rolling, bouncing, or by a combination thereof, resulting in a range of friction values. We evaluated the effect of introducing friction on the shelf by using a relatively low coefficient of sliding friction of 0.1 in the algorithm, which reduced the impact velocity by about 2 m/s and the impact range by about 9 m. The block probably moved over rocky debris or logs on the ramp that acted as rollers or ball bearings, effectively reducing the frictional resistance. The effects of air drag are not as significant as those of friction on the velocity. Depending upon the shape of the block air drag will reduce the impact velocity by about 1 m/s and the impact range will be decreased about 5 m.

Other techniques for calculating the velocity of the block (Haneberg and Bauer, 1993; Pfeiffer et al., 1993) yielded slightly lower results of about 110 m/s at impact. Considering the differences in these various methodologies, including different basic assumptions and data necessary for performing each calculation, and possible, but unknown initial velocity conditions of the block at release, the difference in calculated results of between 110 and 120 m/s are probably not significant.

The length of time between the two impacts from the seismograph record (13.6 s) suggests that the impact of block A could have seismically triggered the failure of block B. If the travel time from release to impact is 12.4 s, as calculated in the algorithm, then the first impact occurred about 1.2 s before the release of block B. If compression (P) and shear (S) waves travel at 6 and 4 km/s, respectively, in granite, and the distance from release to impact is about 850 m (the actual wave path through rock is slightly longer than the point to point travel distance of 820 m partially through the air), then the waves reached the release in about 0.1 and 0.2 s, respectively, about 1 s before the failure of block B. Without knowing prefailure geometry and geologic site conditions, it is not possible to perform a slope stability analysis to determine if the waves were sufficiently strong to have triggered the failure of block B. The postfailure geologic conditions near the release, including multiple (six) major joint sets, joint alteration, and the presence of joint water (Gilliam, 1998), suggest an increased probability of failure during shaking according to a method of assessing regional seismic rock-fall susceptibility by Harp and Noble (1993).

Smaller pieces of the arch fell later that evening and early the next morning (blocks C and D), but these blocks from the southern, thinner end of the arch took a different path than the blocks that had fallen earlier. Instead of sliding on the ramp and then free falling, blocks C and D disaggregated as they followed a chute to the southeast that funneled onto the apex of the talus (Fig. 2).

Figure 3. Rock-fall release (center) and steeply inclined ramp along which blocks slid from left to right before beginning free fall beyond right edge of photograph. Yosemite Valley and Royal Arches are in background. Approximate length of ramp from release (center) to lower right edge of photo is 235 m. (Photograph by Doug Roe, National Park Service.)

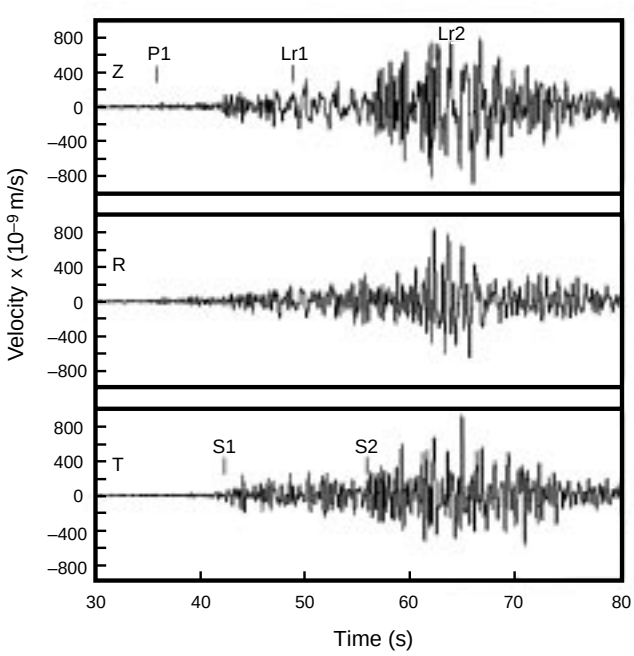

Figure 4. Broadband recordings from a Berkeley Digital Seismic Network station 50 km southeast of the Happy Isles rock-fall impact (from Uhrhammer, 1996). The records have been band-pass filtered from 0.55 to 5.0 Hz, and the horizontal components have been rotated to radial (R) and transverse (T). The top figure shows the vertical component (Z). The prominent phases of the compression wave, P, the shear wave, S, and the Rayleigh wave, L_r recorded on the record are consistent with two impacts A and B, separated in time by 13.6 s. Thus S_1 indicates the time of arrival of the shear wave from the first impact A, and S_2 signifies the shear wave from the second impact B.

Smaller pieces of the arch continued to collapse, slide, and fall during the following days and weeks, continuing until at least early August. A similar period of extended small rock falls continued for about one month after a large rock fall at Middle Brother in the Yosemite Valley (Wieczorek et al., 1995).

AIRBLAST

Ernie Milan, while working on the John Muir Trail, was 360 m east of the impact: he heard a roaring sound, like a jet engine, close overhead, then saw a dark billowy cloud moving slowly and quietly from the impact area on the talus toward the Happy Isles Nature Center. According to a park visitor "there were two big booms, then the cloud started forming." The dust came quickly, enveloping Happy Isles "like a tornado" according to another visitor (Snyder, 1996). Ernie Milan noted that the sky went black for six minutes as the dust raised by the cloud blocked out the late afternoon light. The two booms probably corresponded to impacts A and B, the roaring sound like a jet engine probably the airblast(s) the impact(s) generated.

Impacts A and B generated pressure waves (with compressional and expansion phases) that propagated through the atmosphere away from the source at a rate of at least that of the local atmospheric speed of sound. The leading compression wave was likely a weak shock wave (Anderson, 1984). Trailing the first initial compression wave were expansion and compression waves. These waves created a wind, or airblast, that was comparable in intensity to that of a tornado or hurricane. Like a tornado or hurricane, the airblast intensity is manifested in the type and extent of damage done to structures and vegetation.

The velocity of the airblast was estimated from downed trees using the TORRO Tornado Intensity Scale (Meaden, 1976). The TORRO intensity scale estimates the wind speed of a tornado from the type of damage it caused to buildings and trees. For example, tornadoes with speeds of 120–130 m/s will levitate a house and uproot large trees.

In the seconds before impact B, the local atmosphere may have contained dust from the pulverized rock of impact A. The addition of dust into the atmosphere lowers the speed of sound for pure air (340 m/s). Within 10–20 m from impact B, where trees are completely destroyed, the airblast probably traveled at velocities approaching the speed of sound of the local dusty atmosphere (120–130 m/s). These velocities are consistent with those calculated by a numerical model of the atmospheric dynamic response (velocity, pressure, internal energy, and dust concentration) to the impact (Morrissey et al., 1997). Results of this modeling, more vigorous than that of Kieffer (1981), account for turbulence, heat, and drag effects between the dust and air and suggest that the atmosphere may have contained up to 50% by weight dust prior to impact B.

The most obvious damage inflicted on the forest was uprooting and snapping of about 1000 trees within a 350–500 m radius of the impacts, a process described as windthrow (Fig. 7). The forest is composed of mixed conifers (Douglas fir, incense cedar, yellow [ponderosa] pine, red fir) and broadleaf trees (bigleaf maple, white alder, black oak) ranging from saplings to mature trees 1.5 m in diameter and 40 m tall. Almost all the larger trees toppled in an eastward direction, their roots pulled out.

The major pattern of downed trees formed a radiating, bilaterally symmetrical fan with a central azimuth of 055º–060º, consistent with an airblast from impact B (Fig. 6A). Minor variations on this major pattern along the north edge of downed timber include a few trees downed toward azimuth 080º, which are overlapped by trees of the major pattern (055º–060º). These few trees may have fallen toward azimuth 080º prior to the airblast from impact B. Another variation to the major trend was observed near the south margin where large trees downed toward azimuth 100º are overlain by small trees downed toward 040º. These variations in the patterns of downed trees, which are not particularly well distinguished in Figure 6A, could indicate

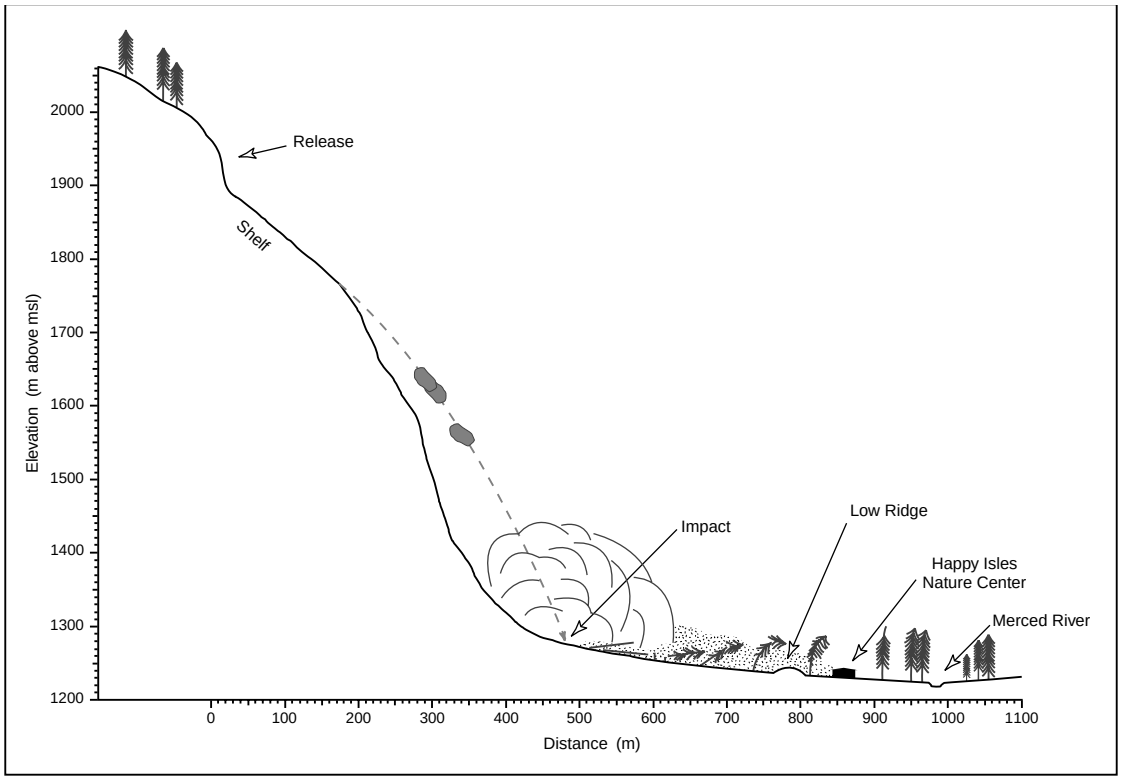

Figure 5. Profile from the rock-fall release (west) to Merced River (east) (msl—mean sea level). Features shown schematically include calculated trajectory of the rock fall, impact, low ridge from prehistoric rock fall, and travel of airblast and sandy cloud toward Happy Isles Nature Center. Note that the initial point of the profile (x = 0) begins 20 m to the west of rock-fall release; consequently, the impact (x = 500) along the profile indicates a distance from release to impact of 480 m.

some nonuniformity in response with respect to the timing or direction of falling trees. Alternatively, the combination of downed tree patterns suggests a possible sequence of events: (1) a relatively small airblast on the north from impact A felled trees eastward (080º); (2) the main blast that radiated from impact B (055º–060º) felled most trees; and (3) a small blast on the south felled trees northeastward (040º) perhaps from later events or rock fall D, or waves redeflected (100º) from impact B by a line of large boulders trending east-west along the southern edge of affected area. These minor variations in the pattern of downed trees are probably not significant in light of the extent and severity of the effects from the major pattern of downed trees from the airblast from impact B.

The effects of the airblast on vegetation varied with direction and distance from the impacts. Near the north edge of the impact B moist soil from springs may have aided the toppling of trees. Near impact A, fallen trees that were either snapped or uprooted lay across one another. In areas near the cliff some of the trees fell by collision with falling or deflected rock: both downed and standing trees are bruised, and many boulder-sized fragments are among them. In contrast, nearly all trees proximal to impact B are uprooted and are aligned in a fan shape in the direction of the Happy Isles Nature Center. The region damaged by the airblast from impact B is roughly triangular with a 50º–60º divergence angle and extends ~500 m downslope from the impact area. Within 20 m of impact, downed trees are found broken into 10–40 cm sections with much bark removed, branches snapped off, and some surfaces impregnated with rock fragments. Timber in this area is discontinuously surrounded by a >35 cm depth of debris composed of rock fragments and sandy dust. At distances of 20–100 m from impact, trunks of fallen trees are in one piece and covered by sandy dust; branches are removed from the upward-facing side and those trees that remain standing have branches that are bent around the trunk.

On surfaces where branches have been snapped off, strips of bark have been removed and sandy debris is wedged beneath the edges of intact bark. On fallen trunks the debarking process apparently occurred after the trees fell, and may have been initiated by ballistic projectiles of rock fragments that splintered patches of bark and were later sheared off by the coarse material in the sandy cloud that followed (Fig. 8). At distances of 100–200 m from impact, fallen trees were uprooted; only a few remained standing, and those had the upper 10–15 m snapped off. Most of the bark remained intact, but the bark was in places splintered, with embedded fragments of rock and tree branches.

At the nature center, about 340 m from impact B, many trees remained standing, a few with their top 10–15 m snapped off at heights roughly equal to that of the roof. The building and adjacent trees may have been somewhat protected from the airblast by a low ridge 70 m upslope with a height at about the same elevation as the roof (Fig. 5). The ridge, created by a prehistoric rock slide, apparently helped to deflect the blast upward, in the process shadowing the nature center. As the blast moved over the ridge, flow separation probably occurred, forming an eddy behind the ridge (Finnigan and Brunet, 1995). Beyond the ridge some of the energy in the airblast dissipated and the few fallen trees crossed each other. Branches and even leaves on low trees up to the height of the ridge were largely intact. Beyond the nature center large fallen trees crushed the snack bar (where the fatality and injuries occurred). A pedestrian bridge about 400 m from impact was also crushed and the Merced River temporarily dammed by a fallen tree. A recording stream gauge showed an instantaneous drop of 10 cm in river level at about the time

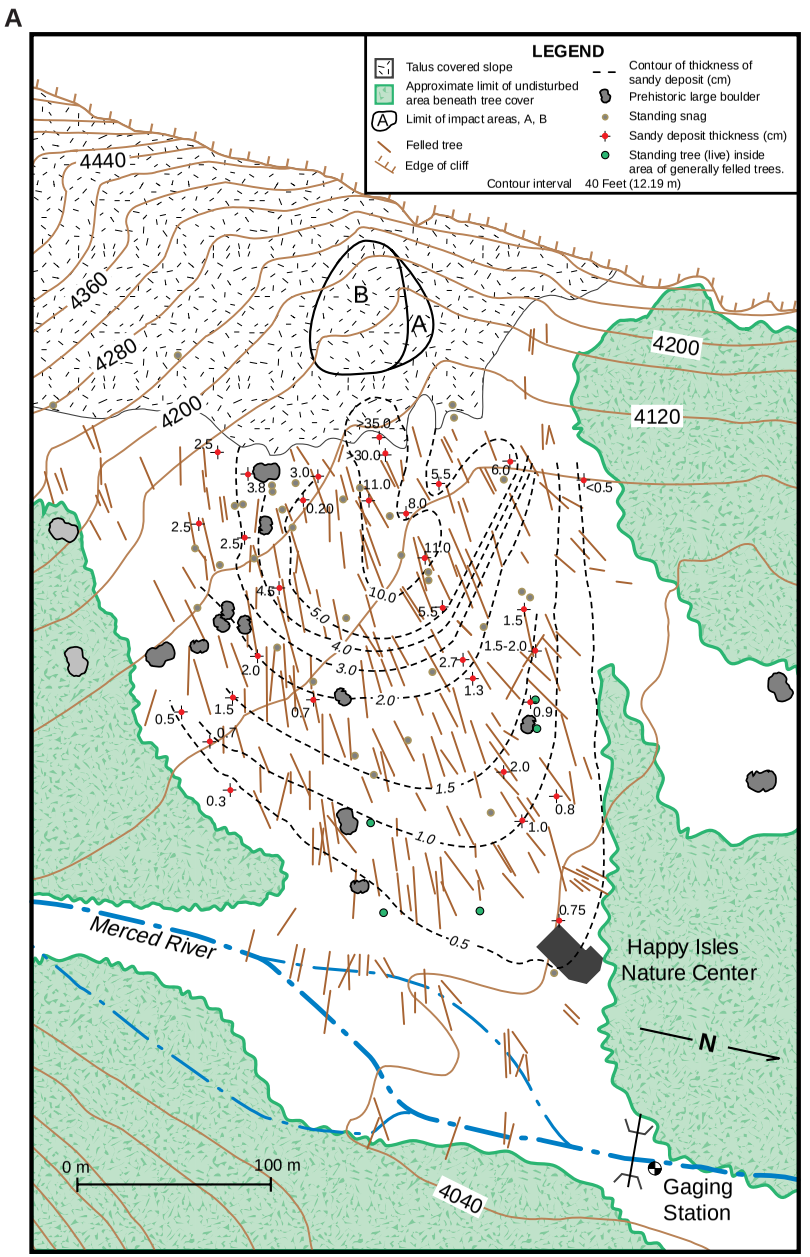

Figure 6. Detailed maps of rock-fall impact area. Location shown in Figure 1. (A) Rock-fall impacts A, B, thickness of deposits from sandy cloud, and downed timber, standing snags, and remaining standing trees near Happy Isles plotted from 1:6600 air photos with Kern PG-2 stereoplotter. Contours of thickness (cm) from sandy-cloud deposits are shown as dashed lines. (B) Map of estimated wind speeds (m/s) of airblast based on damage to vegetation using TORRO scale of categories of wind-speed range (Meaden, 1976). (Photograph used as base by Pacific Aerial Surveys, September 1996.)

Figure 7. Photograph of area damaged by airblast and dense sandy cloud. Trees were uprooted and snapped by airblast. View is east toward Happy Isles Nature Center in distance (center). Snapped trees in foreground approximately 5 m high.

Figure 8. Photograph of splinters caused by coarse sandy gravel blown by dense sandy cloud. Splinters toward top of downed trunk looking away from direction of impact. Note shovel (center) for scale. Shovel is about 1 m long.

of the impact and a rapid recovery within about 10 min, when the flow must have overtopped the blockage by felled trees (Jerry Smithson, U.S. Geological Survey, 1996, written commun.).

The velocity of the airblast dissipated with distance as it encountered trees and boulders (Fig. 6B). The field evidence indicates that most trees were felled by the airblast rather than by impact of debris. For a reconstruction of estimated wind speeds we assumed uniform strength for all types and sizes of trees. Only a few shingles were removed from the roof of the nature center; on the TORRO scale this indicates wind speeds of 17–24 m/s. To the north and west of the building, trees were partially debarked, their branches flagged back, and their tops snapped off, indicative of damage when wind speeds exceed 40 m/s. According to the TORRO scale, where trees were uprooted and partially debarked with most of the branches snapped off, wind speeds apparently reached 84–95 m/s. Nearest to impact B, where trees were completely debarked and snapped into several segments, wind speeds probably exceeded 110 m/s.

A vertical profile of wind speeds in the airblast can be estimated using the TORRO criteria from the number and size of damaged branches as a function of height observed on trees standing at the margins of the devastated area. This velocity profile (Fig. 9) is based on evidence from trees in front of the low ridge about 270 m from impact B. Many of these trees are 25–30-m-tall firs with all twigs and branches removed at heights <12 m. The removal of most branches from trees with bark still intact results from wind speeds of at least 52–61 m/s. At heights from 12 to 20 m, a few large branches remained with a thin cover of needles, indicating wind speeds of 17–24 m/s. Above 20 m in height, the branches in the canopies were densely covered with needles, indicating that the airblast did not extend to this height.

Our field examination showed that the effects of rock falls C and/or D were mostly confined to the preexisting talus and damaged a far smaller area of the surrounding forest and uprooted far fewer trees than the first two rock falls. The main damage is snapped-off tops. Tree tops found near their trunks have 1–3-m-diameter boulders caught between several branches, indicating that the damage was caused by projectiles. Like many rock falls, the absence of larger scale airblast effects from blocks C and D was probably due to splitting of these blocks into pieces during their travel from the release down the chute to the talus (Fig. 2).

DENSE SANDY CLOUD

A dense sandy cloud, similar in some dynamic and sedimentologic respects to a pyroclastic flow, shortly followed the airblast, scoured overturned trees, and left behind deposits of gravelly sand. Most of the sand was fragmented and pulverized material produced by the impact. Grain-size characteristics indicate that the rock fall pulverized into constituent mineral grains of medium- to fine-sand size of 0.5–0.125 mm (1 –3 ϕ) (Fig. 10A). Within the areas of impacts A and B, few pieces larger than 1–2 m remained and some boulders had been so weakened by the impact that they could be split apart by hand.

Sandy deposits were observed within the main area of disturbance as far as 350 m from impact B; their thickness is contoured in Figure 6A. In the proximal area (within 100 m of the east edge of impact B), the sandy deposits are as thick as 35 cm and decrease outward axially and laterally to only a few millimeters near the outer edge of the downed timber. The thin distal deposits grade out well beyond this area of devastation, becoming only several millimeters thick and difficult to measure consistently amid vegetation. The mean grain size decreases outward systematically due to the diminishing size and abundance of coarse clasts (Fig. 10B). Some coarse clasts in the proximal area may be attributed to projectiles from impact rather than entrainment in the cloud. If gravel-sized clasts are ignored, however, the mean size of the sand fraction also grades to finer size outward. All samples are very poorly sorted, improving somewhat outward inversely with mean grain size as the coarser clasts diminish.

The relative timings of the airblast and cloud in the proximal area are indicated by downed trees having remarkably little damaged bark, while the undersides (facing the impact) of their root balls are heavily battered and abraded. This pattern is universal in the proximal area. Although slower than

the airblast, the sandy cloud moved fast enough to abrade trees that had been debarked by the airblast. As described earlier, projectile impacts splintered the bark and peeled it back in the direction the tree had fallen (Fig. 8).

Beyond the proximal area (>100 m from impact B), most of the root balls of uprooted trees were unabraided; even the undersides of the roots retained their bark. Limber, smaller trees (<20 cm diameter) remained standing but had their branches stripped, were bowed convex upward and tilted in the direction of fallen trees. Even smaller saplings (<10 cm diameter) were limber enough to retain many branches but were tilted and entirely stripped of leaves. The abrasion and bending of branches on downed trees clearly occurred after the airblast passed through. Tree abrasion decreased distally, recording an outward-decreasing velocity of the sandy cloud, as does the outwardly smaller grain size.

The travel and expansion of the sandy cloud triggered by the rock-fall impact were photographed and videotaped. The cloud, initially quite small near the impact, expanded as it traveled downslope toward the Nature Center. The cloud had an opaque, off-white, cauliflower form like those of vigorous, gravity driven, ground-hugging flows such as volcanic density currents (pyroclastic flows and surges) (Bursik et al., 1992). The cloud surged across the valley and climbed the south side of Grizzly Peak to a height nearly equal to that of the release (Fig. 11). The velocity of the cloud was measured using reference points such as waterfalls in the background and the estimated time between frames of the videotape. The displacement of the cloud was measured to be initially traveling at a rate of about 1 m/s, then accelerating to nearly 5 m/s, much slower than the airblast. This measurement supports trail worker Ernie Milan's description of a cloud moving slowly from the impact area toward the Happy Isles Nature Center. Although dust clouds generated by rock falls are not unusual (Snyder, 1996), the distance that the cloud traveled and its coarse abrasive nature is unusual.

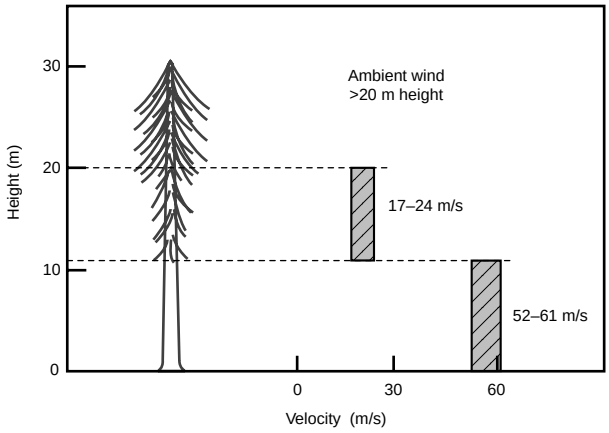

Figure 9. Estimated vertical profile of wind speeds in airblast about 270 m from the impact B based on damage to vegetation using TORRO scale of categories of wind speed range (Meaden, 1976).

DISCUSSION

Wind gusts initiated by snow avalanches can down trees, move structures, and carry away people (Heim, 1932). Airblasts generated by rock falls or rock avalanches are rarely observed (Table 1). Eyewitnesses to a large rock avalanche in 1883 near Elm, Switzerland, noted a blast of air and dust ahead of the rock avalanche; this airblast even pushed some people to safety (Heim, 1932). The 1959 Madison Canyon, Montana, landslide generated an airblast strong enough to topple and roll an automobile and to move two people (Hadley, 1978). The 1970 fall of rock and ice from Nevados Huascarán in Peru fragmented into a debris avalanche behind a wind strong enough to throw people to the ground and to topple trees near the debris margin. The wind carried "mud" abrasive to the skin (Plafker and Ericksen, 1978), perhaps a sandy cloud behind an airblast similar to that at Happy Isles.

Rock falls or rock avalanches that have generated airblasts (Table 1) commonly attained high velocities through a segment of airborne free fall. The airblast or wind observed in these cases may reflect the displacement of air by a large rapidly moving mass. The height of free fall and hence the velocity of the rock fall at impact appear to influence the severity of the airblast.

Explosive volcanic eruptions can generate pyroclastic surges, similar somewhat in dynamics and sedimentology to the airblast and dense sandy cloud observed at Happy Isles. The abrasive, hot, ground- hugging, pyroclastic surge from Mount St. Helens on May 18, 1980, downed timber and overturned vehicles as it moved downslope by gravity at an average speed of 55 m/s as far as 25 km from the vent (Waitt, 1981). Like the dense sandy cloud at Happy Isles, the Mount St. Helens surge splintered, abraded, and sandblasted trees (Moore and Sisson, 1981).

Geologic and topographic factors influence the generation of airblasts by rock falls in Yosemite. Rock masses with widely spaced and oriented joints that favor the development of overhanging arch-like structures of rock can detach and become airborne with little internal disruption. The 1996 Happy Isles and 1872 Liberty Cap rock falls at Yosemite are among the smallest documented rock falls to have triggered airblasts (Table 1). The shape or surface area of the falling rock mass may influence the generation of an airblast; slab-shaped structures are more likely to trap and expel air at impact than more equidimensional pieces. Judging from the geometry at their release, and photographs of prefailure formations, the Happy Isles and Liberty Cap rock falls were of elongate, thin sheets of rock.

Topography conducive to a large vertical drop of falling masses without intervening impacts along the slope influences the generation of airblasts. The slope profile of a rock fall is important; near-vertical paths minimize impacts and disruption of the rock mass more than gentler slopes. The estimated velocity of the Happy Isles rock fall, 110–120 m/s, was among the highest of those documented triggering airblasts (Table 1). A rock fall from Middle Brother in Yosemite Valley was larger and had a higher relative elevation than the Happy Isles rock fall, but did not generate a strong airblast (Snyder, 1996). The blocks at Middle Brother broke into many pieces from impacts while traveling to the valley floor. The Happy Isles rock fall became airborne with enough horizontal velocity to clear the base of the cliff, thus probably remaining intact and accelerating to a high velocity at impact. The trajectories of blocks A and B were due to a favorably oriented and inclined ramp above a steep cliff shaped by previous glaciations. These geologic and topographic conditions are not necessarily unique to Yosemite. Other high relief glacially oversteepened valleys and mountainous areas susceptible to rock falls may generate unusual effects such as airblasts and abrasive dense sandy clouds. The unusual effects of this rock fall illustrate the importance of considering collateral geological hazards in planning development in mountainous regions.

ACKNOWLEDGMENTS

Morrissey's work on the analysis of the airblast was supported by the U.S. Geological Survey. Richard Waitt interpreted the patterns of downed timber and the deposits left by the sandy cloud. Robert Uhrhammer analyzed the seismographs of the rock-fall impacts and developed the algorithm for calculating the velocity of the rock fall. Marcus Bursik and Lee Finewood analyzed video film to constrain the velocity of the sandy cloud. James Snyder, Robert Norris, and Edwin Harp assisted with field interpretation of the rock-fall events.

In their reviews of this paper William Haneberg performed an alternative

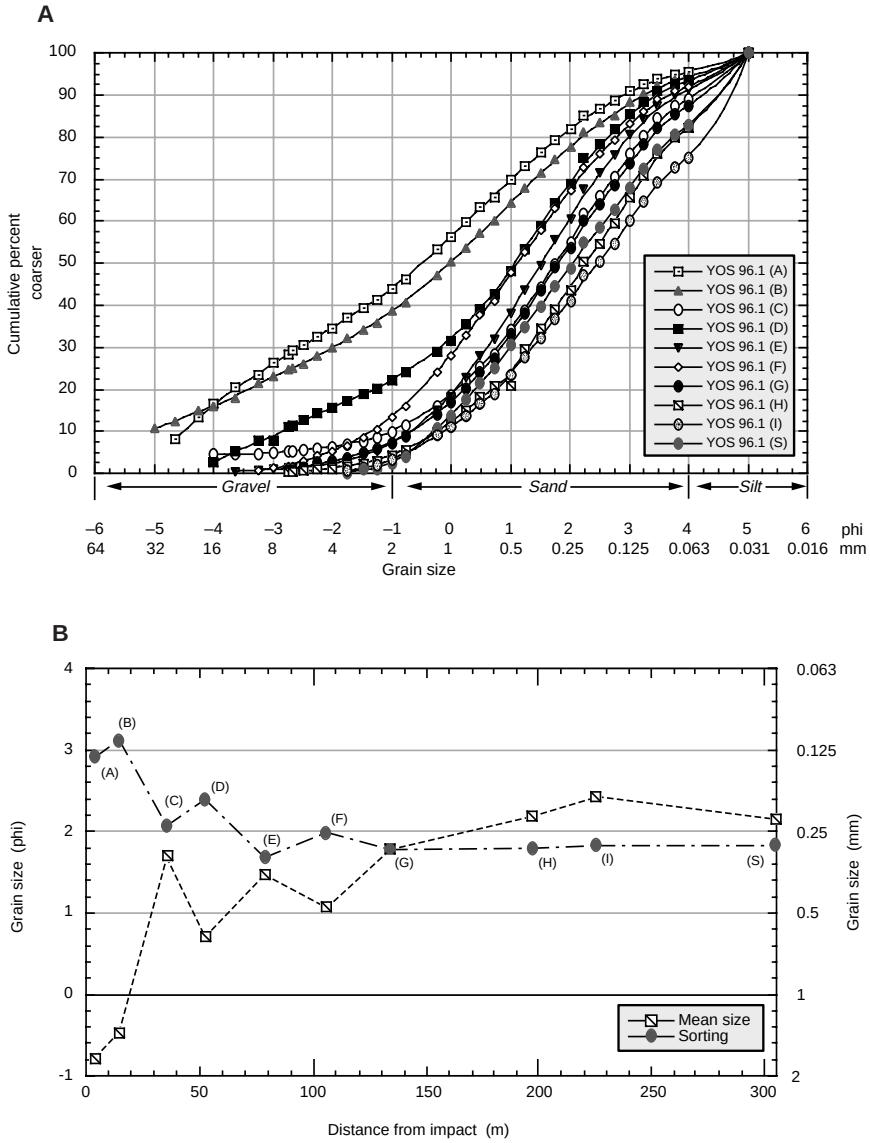

Figure 10. Grain-size characteristics of sandy cloud. (A) Summary of grain-size distribution of deposits from samples taken along approximate central flow path from edge of impact B to Happy Isles Nature Center. Pan fraction (finer than 4ϕ) is unanalyzed and arbitrarily plotted at 5ϕ for all samples. (B) Mean particle size and sorting as a function of distance from impact. Mean is Folk's (1974) graphic mean (M_z), sorting Folk's inclusive graphic standard deviation (σ_I).

analysis to determine the velocity of the rock fall and Richard Iverson made worthwhile comments that resulted in significant improvements. Sarina Lambert and Jack Phinney of the National Park Service assisted with the collection of samples of sandy deposits. David Walter provided his series of photographs of the cloud following impact. Dan Gilliam, graduate student at Radford University, conducted studies of the rock-fall release area. Several colleagues at the U.S. Geological Survey assisted with this study: Rex Baum supervised the geotechnical laboratory work, Chris Catherman prepared graphic imagery, Lou Thompson developed photography, and John Unger, George Plafker, and King Huber reviewed early versions of the paper.

APPENDIX. ALGORITHM FOR VELOCITY OF ROCK FALL

Trajectory Program

```
c
c..... calculate rock trajectory assuming frictionless shelf
c       and no air drag
c
        implicit none
        integer*4 I, n
        real*8 xx(10000), zz(10000)
        real*8 g, dt, z, x, v_z, v_x, t, g_z, g_x, v, theta, angle
c
        open(10,file='YRF_prof_meters.data',status='old')
        I=0
    1 I=I+1
        read(10,'(2f10.3)',end=2) xx(I),zz(I)
c
c..... assume that release is centered at 1940 m elevation
c
        if(zz(I).gt.1940.d0) then
        I=I-1
        endif
        go to 1
    2 n=I-1
        close(10)
```

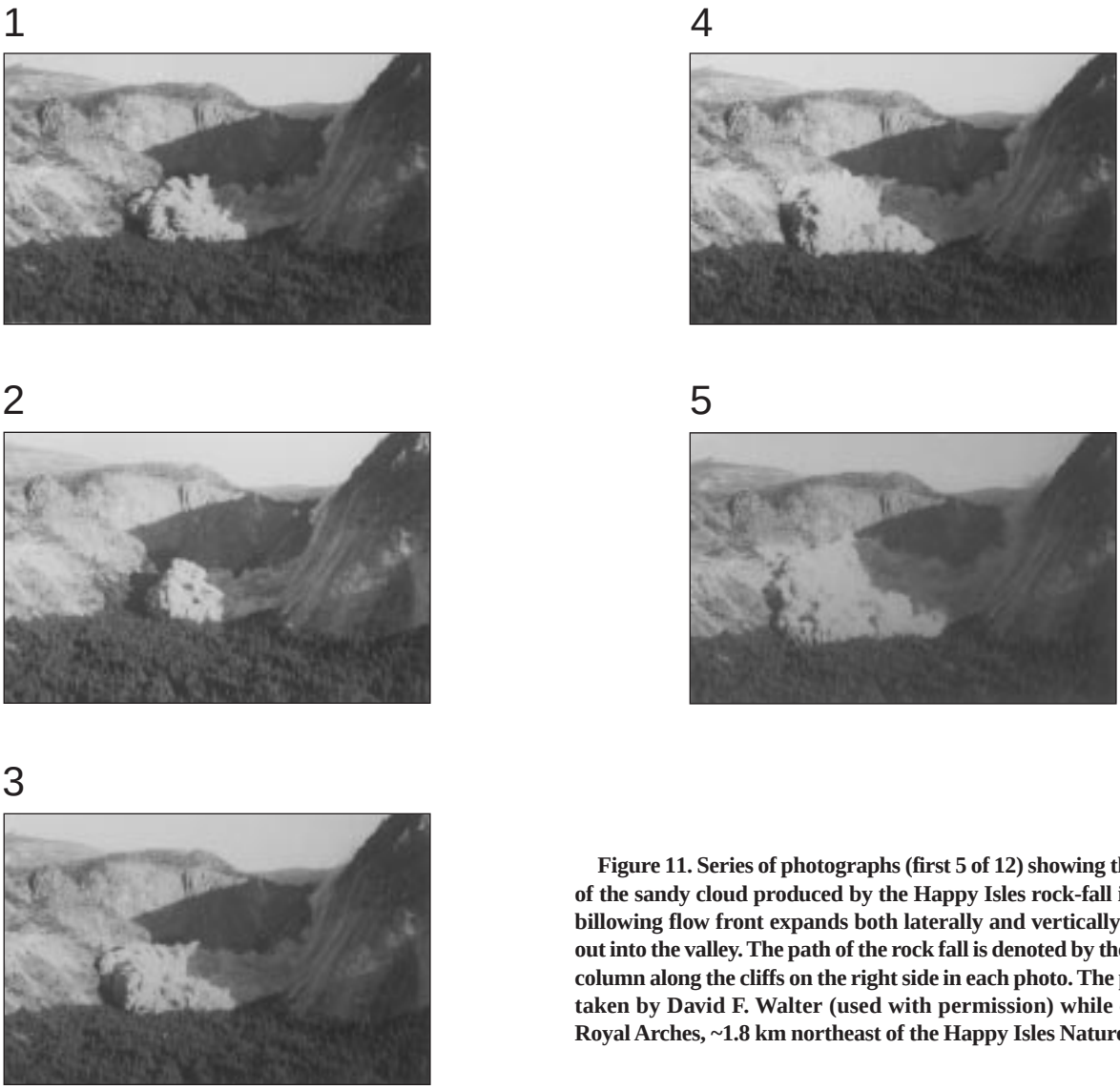

Figure 11. Series of photographs (first 5 of 12) showing the evolution of the sandy cloud produced by the Happy Isles rock-fall impact. The billowing flow front expands both laterally and vertically as it moves out into the valley. The path of the rock fall is denoted by the rising dust column along the cliffs on the right side in each photo. The photos were taken by David F. Walter (used with permission) while climbing at Royal Arches, ~1.8 km northeast of the Happy Isles Nature Center.

TABLE 1. ROCK FALL CHARACTERISTICS AND AIRBLAST EFFECTS

Rock fall	Volume (10^6 m^3)	Height of fall (m)	Velocity (m/s)	Airblast effects	Source
Goldau, Switzerland (1806)	30–40	1040	40*–70*	Herdsman and goats picked up and whirled into the air; four children picked up into the air	Heim (1932)
Nevados Huascarán, Peru (1970)	50–100	600†	78*–>200	People knocked down; many wind-toppled large trees, leaves stripped from trees and brush; airblast with abrasive mud stripped vegetation and abraded skin	Plafker and Ericksen (1978)
Elm, Switzerland (1882)	10	570	50*–100	Several people lifted into the air and carried; well-constructed wooden houses lifted; trees bent	Heim (1932)
Happy Isles, California (1996)	0.03	550	110–120	About 1000 trees toppled and snapped; branches bent; abrasive sandy cloud stripped bark and vegetation	This report
Liberty Cap, California (1872)	0.04	275	70	Collapsed weak structure; slightly moved another well-constructed building; knocked man to ground	Wieczorek et al. (1992)
Los Chocoyos, Guatemala (1976)	1.2	100	>28	Bent a few small trees, moved blocks of adobe and road pavement	Harp et al. (1981)
Madison Canyon, Montana (1959)	21	90	50	Tumbled car, lifted and carried two people into the air	Hadley (1978)

Note: Rock-fall velocities are estimated by several methods, hence comparisons are only approximate.
*These reported values should be considered as average velocities.
†Distance of initial free fall of rock and ice from west face of Nevados Huascarán. From below the west face the debris accelerated down Glacier 511 for a slope distance of 2.4 km with a vertical drop of nearly 1 km, with parts of the debris becoming air launched near the base of the glacier (Plafker and Ericksen, 1978).

TABLE A1. RESULTS OF VELOCITY ALGORITHM

X* (m)	V_X (m/s)	A_X (m/s_2)	Z (m)	V_Z (m/s)	A_Z (m/s^2)	Angle† (°)	V (m/s)	T (s)
20.5	0.0	2.5	1940	–0.0	–9.5	75.4	0.0	0.001
84.8	46.9	7.6	1850	–37.8	–6.2	38.9	60.2	4.412
180.8	52.2	7.1	1768	–49.8	–6.8	43.6	72.1	6.285
180.9	52.2	0.0	1767	–49.8	–9.8	43.6	72.2	6.286
244.5	52.2	0.0	1700	–61.7	–9.8	49.7	80.9	7.504
320.4	52.2	0.0	1600	–75.9	–9.8	55.5	92.2	8.957
384.2	52.2	0.0	1500	–87.9	–9.8	59.3	102.3	10.177
440.3	52.2	0.0	1400	–98.4	–9.8	62.0	111.4	11.251
490.9	52.2	0.0	1300	–107.9	–9.8	64.2	119.9	12.220
500.5	52.2	0.0	1280	–109.7	–9.8	64.5	121.5	12.404
502.9	52.2	0.0	1275	–110.2	–9.8	64.6	121.9	12.449

Note: See Appendix for definition of variables.
*The range of the rock fall starting from the release.
†The trajectory angle measured from horizontal.

```
c
            g=9.8d0
            dt=0.001d0
            z=zz(1)
            x=xx(1)
            v_z=0.d0
            v_x=0.d0
            t=0.d0
            I=1
   3 I=I+1
            if(i.gt.n) go to 5
c
c….. assume that rock goes ballistic at 1768 m elevation
c
            if(z.gt.1768.0d0) then
             theta=datand((xx(I)-xx(I-1))/(zz(I-1)-zz(I)))
             g_z=-g*0.90d0*dcosd(theta)
             g_x= g*0.90d0*dsind(theta)
            else
            g_z=-g
            g_x=0.d0
            endif
   4 t=t+dt
c
c….. assume impact occurs above 1270 m elevation
c
            if(z.lt.1270.d0) go to 5
            v_z=v_z+g_z*dt
            z=z+v_z*dt
            if(z.gt.1768.d0) then
             v_x =-v_z*dtand(theta)
            endif
            x=x+v_x*dt
            v=dsqrt(v_x*v_x+v_z*v_z)
            angle=datan2d(-v_z,v_x)
            write(*,'(9f10.3)') x, v_x, g_x, z, v_z, g_z, angle, v, t
            if(z.lt.1270.d0) go to 5
            if(z.lt.zz(I+1)) go to 3
            go to 4
   5 continue
c
            stop
            end
```

Where:
x = range in meters
v_x = x velocity
a_x = x acceleration
z = elevation in meters
v_z = z velocity
a_z = z acceleration
angle = trajectory angle from horizontal

REFERENCES CITED

Alpha, T. R., Wahrhaftig, C., and Huber, N. K., 1987, Oblique map showing maximum extent of 20,000-year-old (Tioga) glaciers, Yosemite National Park, Central Sierra Nevada, California: U.S. Geological Survey Miscellaneous Investigations Series Map I-1885, 1 sheet.

Anderson, J. D., 1984, Fundamentals of aerodynamics: New York, McGraw-Hill, 563 p.

Bursik, M. I., Sparks, R. J. S., Carey, S. N., and Gilbert, J. S., 1992, Sedimentation of tephra by volcanic plumes, I. Theory and its comparison with a study of the Fogo A Plinian deposit Sao Miguel (Azores): Bulletin of Volcanology, v. 54, p. 329–344.

Finnigan, J. J., and Brunet, Y., 1995, Turbulent airflow in forests on flat and hilly terrain, *in* Coutts, M. P., and Grace, J., eds., Wind and trees: Cambridge, Cambridge University Press, p. 3–39.

Folk, R. L., 1974, Petrology of sedimentary rocks: Austin, Texas, Hemphill Publishing Co., 182 p.

Gilliam, D. R., 1998, A structural and mechanical analysis of the Happy Isles rockfall, July 10, 1996, Yosemite National Park, Mariposa County, California [Master's thesis]: Radford, Virginia, Radford University, 172 p.

Hadley, J. B., 1978, Madison Canyon rockslide, Montana, U.S.A., *in* Voight, B., ed., Rockslides and avalanches, 1 Natural phenomena: New York, Elsevier, p. 167–180.

Haneberg, W. C., and Bauer, P. W., 1993, Geologic setting and dynamics of a rockslide along NM 68, Rio Grande Gorge, New Mexico: Association of Engineering Geologists Bulletin, v. 30, p. 7–16.

Harp, E. L., and Noble, M. A., 1993, An engineering rock classification to evaluate seismic rock-fall susceptibility and its application to the Wasatch Front: Association of Engineering Geologists Bulletin, v. 30, p. 293–319.

Harp, E. L., Wilson, R. C., and Wieczorek, G. F., 1981, Landslides from the February 4, 1976, Guatemala earthquake: U.S. Geological Survey Professional Paper 1204-A, 35 p.

Heim, A., 1932, Landslides and human lives (Bergsturz und Menschenleben: Skermer, N., translator, 1989): Vancouver, B.C., BiTech Publishers Ltd., 195 p.

Huber, N. K., 1987, The geologic story of Yosemite National Park: U.S. Geological Survey Bulletin 1595, 64 p.

Kieffer, S. W., 1981, Fluid dynamics of the May 18 blast at Mount St. Helens, *in* Lipman, P. W., and Mullineaux, D. R., eds., The 1980 eruptions of Mount St. Helens, Washington: U.S. Geological Survey Professional Paper 1250, p. 379–400.

Matthes, F. E., 1930, Geologic history of the Yosemite Valley: U.S. Geological Survey Professional Paper 160, 137 p.

Meaden, G. T., 1976, Tornadoes in Britain: Their intensities and distribution in space and time: Journal of Meteorology, v. 1, p. 242–251.

Moore, J. G., and Sisson, T. W., 1981, Deposits and effects of the May 18 pyroclastic surge, *in* Lipman, P. W., and Mullineaux, D. R., eds., The 1980 eruptions of Mount St. Helens, Washington: U.S. Geological Survey Professional Paper 1250, p. 421–438.

Morrissey, M. M., Wieczorek, G. F., and Savage, W. Z., 1997, Airblasts generated from rock-fall impacts: The 1996 Happy Isles rock fall, Yosemite National Park [abs.]: Eos (Transactions, American Geophysical Union), v. 78, p. 46, p. F137.

Norris, R. D., 1994, Seismicity of rockfalls and avalanches at three Cascade Range volcanoes; implications for seismic detection of hazardous mass movements: Seismological Society of America Bulletin, v. 84, p. 1425–1939.

Pfeiffer, T. J., Higgins, J. D., Andrew, R. D., Barrett, R. K., and Beck, R. B., 1993, Colorado rockfall simulation program—Users manual for version 3.0: Colorado Department of Transportation Report CDOT-DTD-ED3-CS-2B, 66 p.

Plafker, G., and Ericksen, G. E., 1978, Nevados Huascarán avalanches, Peru, *in* Voight, B., ed., Rockslides and avalanches, 1 Natural phenomena: New York, Elsevier, p. 277–314.

Snyder, J., 1996, The ground shook and the sky fell: Yosemite Association, Fall 1996, v. 58, no. 4, p. 2–9.

Uhrhammer, R. A., 1996, Yosemite rock fall of July 10, 1996: Seismological Research Letters, v. 67, p. 47–48.

Waitt, R. B., 1981, Devastating pyroclastic density flow and attendant air fall of May 18—Stratigraphy and sedimentology of deposits, *in* Lipman, P. W., and Mullineaux, D. R., eds., The 1980 eruptions of Mount St. Helens, Washington: U.S. Geological Survey Professional Paper 1250, p. 439–458.

Wieczorek, G. F., and Jäger, S., 1996, Triggering mechanisms and depositional rates of postglacial slope-movement processes in the Yosemite Valley, California: Geomorphology, v. 15, p. 17–31.

Wieczorek, G. F., Snyder, J. B., Alger, C. S., and Isaacson, K. A., 1992, Rock falls in Yosemite Valley, California: U.S. Geological Survey Open-File Report 92–387, 38 p.

Wieczorek, G. F., Nishenko, S. P., and Varnes, D. J., 1995, Analysis of rock falls in the Yosemite Valley, California, *in* Daemen, J. J., and Schultz, R. A., eds., Proceedings, Rock Mechanics Symposium, 35th, Reno, Nevada: Rotterdam, Balkema, p. 85–89.

MANUSCRIPT RECEIVED BY THE SOCIETY OCTOBER 16, 1997
REVISED MANUSCRIPT RECEIVED NOVEMBER 24, 1998
MANUSCRIPT ACCEPTED FEBRUARY 12, 1999

Printed in U.S.A.